Published in final edited form as:
Cell Mol Life Sci. 2012 February ; 69(4): 641–650. doi:10.1007/s00018-011-0771-x.

Chromatin affinity-precipitation using a small metabolic molecule: its application to analysis of *O*-acetyl-ADP-ribose

Shu-Yun Tung,
Institute of Molecular Biology, Academia Sinica, Taipei 11529, Taiwan, ROC

Jia-Yang Hong,
Institute of Molecular and Genomic Medicine, National Health Research Institutes, Miaoli 35053, Taiwan, ROC

Thomas Walz,
Department of Cell Biology, Harvard Medical School, Boston, MA 02115, USA, Howard Hughes Medical Institute, Harvard Medical School, Boston, MA 02115, USA

Danesh Moazed, and
Department of Cell Biology, Harvard Medical School, Boston, MA 02115, USA, Howard Hughes Medical Institute, Harvard Medical School, Boston, MA 02115, USA

Gunn-Guang Liou
Department of Cell Biology, Harvard Medical School, Boston, MA 02115, USA, Institute of Molecular and Genomic Medicine, National Health Research Institutes, Miaoli 35053, Taiwan, ROC

Danesh Moazed: danesh@hms.harvard.edu; Gunn-Guang Liou: bogun@nhri.org.tw

Abstract

In the cell, many small endogenous metabolic molecules are involved in distinct cellular functions such as modulation of chromatin structure and regulation of gene expression. *O*-acetyl-ADP-ribose (AAR) is a small metabolic molecule that is generated during NAD-dependent deacetylation by Sir2. Sir2 regulates gene expression, DNA repair, and genome stability. Here, we developed a novel chromatin affinity-precipitation (ChAP) method to detect the chromatin fragments at which small molecules interact with binding partners. We used this method to demonstrate that AAR associated with heterochromatin. Moreover, we applied the ChAP method to whole genome tiling array chips to compare the association of AAR and Sir2. We found that AAR and Sir2 displayed similar genomic binding patterns. Furthermore, we identified 312 potential association cluster regions of AAR. The ChAP assay may therefore be a generally useful strategy to study the small molecule association with chromosomal regions. Our results further suggest that the small metabolic molecule AAR associates with silent chromatin regions in a Sir2-dependent manner and provide additional support for the role of AAR in assembly of silent chromatin.

Correspondence to: Danesh Moazed, danesh@hms.harvard.edu; Gunn-Guang Liou, bogun@nhri.org.tw.

Electronic supplementary material The online version of this article (doi:10.1007/s00018-011-0771-x) contains supplementary material, which is available to authorized users.

Keywords

Chromatin affinity-precipitation (ChAP); *O*-acetyl-ADP-ribose (AAR, OAADPR); Sir2; Chromatin immunoprecipitation (ChIP); Silent chromatin

Introduction

In addition to proteins, many noncoding RNA molecules and small metabolites, such as NAD, GTP, ADPR, NAM, and cAMP, may play important regulatory roles in the cell. Similar to the widely studied small noncoding RNA molecules, which are involved in the regulation of gene expression, small cellular metabolites and biosynthetic molecules, such as cAMP, tRNATyr, FMN, and NAD, play important roles in modulation of gene expression in the cell [16, 25, 53]. These small regulatory molecules are involved in either changing the activity of transcription factors/cofactors [16, 55], the feedback loop of transcriptional RNA level [12, 32], or changes in chromatin structure [25, 30, 39]. Therefore, small metabolic molecules might be also involved in epigenetic processes. However, although some metabolites have been well studied and have well-known biological functions and mechanisms, many remain poorly characterized and the details of their molecular mechanisms, even their fundamental biological functions, still remain to be determined.

O-acetyl-ADP-ribose (OAADPR or AAR for simplicity) is a small metabolic molecule. The cellular AAR concentration has been reported to be around 560 nM [27]. AAR is generated during NAD-dependent deacetylation by silent information regulator 2 (Sir2) family proteins [4, 5, 30, 38, 44, 48]. Sir2 is involved in many distinct cellular functions, including the regulation of gene expression, genome stability, metabolism, and aging [4, 8, 13, 21, 26, 33, 37, 42, 44, 46, 49, 52, 53]. There are several other AAR-producing enzymes, such as Hst1, in the cell. Although AAR is produced by Sir2-like proteins from bacteria, yeast, and humans and is shown to block/delay oocyte maturation [5], bind to chromatin-related proteins [24], activate ion channels [15], and affect cellular reduction-oxidation status [51], its precise biological functions and molecular mechanisms are not fully known.

In eukaryotic cells, nuclear DNA is packaged into chromatin. Post-translational modifications of histones and association with histone-binding proteins organize the genome into distinct states that are referred to as heterochromatin and euchromatin [22, 33, 40]. The known heterochromatic DNA domains of *Saccharomyces cerevisiae* are the silent mating type loci (*HML* and *HMR*) and the telomeric DNA regions [33, 43]. In addition, silencing factors are involved in stabilization of the ribosomal DNA (rDNA) tandem repeats [6, 45]. The Sir proteins, Sir2, Sir3, and Sir4, are required for establishing and maintaining silent chromatin domains at telomeres and the mating type loci [1, 14, 23, 41]. These Sir proteins form a nucleosome binding complex called the SIR complex [34–36, 47]. AAR has been shown to promote a change in stoichiometry and structure of the SIR complex in vitro [30]. In addition, NAD-dependent deacetylation of nucleosome arrays purified from yeast, coupled to AAR synthesis, results in the formation of SIR-nucleosome filaments that require all three Sir proteins [39]. Because binding of the SIR complex to nucleosome arrays in these experiments is not sufficient for filament formation, we proposed that AAR induces a structural change that mediates filament formation. These results suggest that AAR binds to at least one of the Sir proteins and indicate that both deacetylation and AAR synthesis contribute to SIR complex assembly in vitro and that both events may be required for the formation of silent chromatin in vivo. In addition, AAR increases the affinity of the Sir3 protein for nucleosomes in in vitro binding assays [31]. However, it has been reported that the requirement for Sir2 and AAR can be partially bypassed in some transcriptional silencing assays [9, 54].

In this study, we developed a novel chromatin affinity-precipitation (ChAP) method, which allowed us to study the ability of immobilized small molecules to precipitate specific chromatin fragments. Using AAR as an example, the results demonstrated that AAR associated with silent heterochromatic regions in a Sir2-dependent manner. Moreover, we used the ChAP method to compare the association of AAR and Sir2 via high resolution whole genome tiling array chips. We found that AAR displayed a similar genomic binding pattern to that of Sir2. We also identified 312 additional association cluster regions for AAR. These results indicate that AAR can associate with specific target(s) in silent chromatin and establish ChAP as a general method for probing the chromosomal targets of metabolites.

Materials and methods

Yeast strains

The yeast strains used for this study were SF10 (BJ459, *MAT*a *ura3-52 trp1 lys2-801 leu2Δ1 pep4Δ::HIS3 prb1Δ1.6R can1*) and W303-1a (*MAT*a *ade2-1 can1-100 his3-11,15 leu2-3,112 trp1-1 ura3-1*). Strain *sir2Δ::HIS3* (JRY3433) was previously described [34, 42].

Purification of proteins and ^{32}P-*O*-acetyl-ADP-ribose (AAR), gel electrophoresis, Western blotting, quantification, and HDAC fluorescent activity assay

Proteins were purified as previously described [30, 35]. ^{32}P-AAR was prepared by deacetylation of an acetylated histone H4 peptide using Hst2 and ^{32}P-NAD. Protein samples were separated on SDS-PAGE and stained by Coomassie brilliant blue R520 or silver nitrate to visualize protein bands. Western blotting was performed using either the ECL Western blot detection system (Amersham Biosciences) or the Western Lightning Chemiluminescence Reagent (PerkinElmer Life Sciences). AlphaEaseFc (Alpha Innotech) was used to quantify the density of protein or DNA bands on the gel and of small molecule spots on the TLC plate. HDAC fluorescent activity assay was performed following the manufacturer's instructions (Merck/Biovision kit) except a reaction buffer containing 1 mM NAD was used. Briefly, 85 μl of enzyme was mixed with 10 μl of HDAC assay reaction buffer and added to 5 μl of fluorescent substrate. After 30 min incubation at 37°C, the reaction was stopped by adding 10 μl of lysine developer and incubation at 37°C for 30 min. The signals were recorded by reading samples in a fluorescence plate reader (Ex/Em: 350–380/440–460 nm).

Deacetylation reactions, TLC, HPLC, and MALDI-TOF mass spectrometry

Approximately 2.5 mg GST-Sir2 was immobilized on glutathione-Sepharose 4B (Amersham Biosciences). The immobilized GST-Sir2 was incubated with 1 mM β-NAD$^+$ and 1.5 mM synthetic penta-acetylated histone H4 peptide (SGRGK^{Ac}GGK^{Ac}GLGK^{Ac}GGAK^{Ac}RHRK^{Ac}, Yao-Hong Biotechnology) in 1.75 ml of 50 mM HEPES-KOH (pH 7.0), 300 mM KCl, 1 mM $Mg(OAc)_2$ for 2 h at 30°C and then overnight at 4°C. Protein bound to the solid beads was packaged into a column, and the enzymatic reaction products were eluted and either directly tested by TLC or further analyzed by HPLC and MALDI-TOF mass spectrometry using standard procedures as previously described [30].

Dot blotting

Serial dilutions of protein samples were spotted on a PVDF membrane (50–200 μmol) and were incubated with ^{32}P-AAR at 4°C overnight. The membranes were then washed twice with 20 mM Hepes-KOH pH 8.0, 300 mM KCl, 1 mM $MgCl_2$, and 0.05% NP40, followed by two washes with 20 mM Hepes-KOH pH 8.0, 100 mM KCl, 1 mM $MgCl_2$, and 0.025%

NP40 at room temperature. The membranes were then subjected to autoradiography and quantification by phosphorimaging using QuantityOne software (BioRad).

BIAcore surface plasmon resonance analysis

Real time protein-small molecule interactions were examined using a BIAcore 3000 or BIAcore 2000 instrument (BIAcore). Sir2 or BSA was individually immobilized on different flow cell of a CM5 sensor chip using an amine-coupling kit (BIAcore). The experimental procedures for interaction assays and data analysis were previously described [29, 30].

Affinity pull-down and chromatin affinity-precipitation (ChAP)

Activated Affigel 10 resin (BioRad) was washed with ice cold H_2O three times and equilibrated in cold buffer A (50 mM Hepes-KOH pH 8.0, 300 mM KCl, 1 mM $MgCl_2$, 0.05% NP40, 0.5% BSA, 0.5% casamino acids) three times. To immobilize a small molecule on the beads, 10 mM individual NAD, ADPR, NAM, AAR, ATP, ADP, or AMP was coupled to the beads at 4°C for 4–6 h, followed by washes with cold buffer B (50 mM Tris-HCl pH 7.0, 150 mM KCl, 1 mM $MgCl_2$, 0.05% NP40, 0.1% BSA, 0.5% casamino acid) three times. To block the remaining coupling sites, cold 1 M ethanol-amine-HCl pH 8.5 was incubated with beads for 1–2 h. The beads were then washed with cold buffer B three times.

For affinity pull-down assays, purified protein or whole cell lysate extract, containing 0.1% BSA and 0.1% casamino acid, was added to each immobilized resin and incubated at 4°C overnight. Before elution with buffer C (4× SDS-PAGE Laemmli loading dye without Bromo-phenol blue), beads were washed five times with cold buffer B.

For ChAP, the treatment of cell lysate extract was as previously described for ChIP assays [39]. Each immobilized resin was incubated with cell lysate at 4°C overnight. Beads were then washed once with cell lysis buffer (50 mM Hepes-KOH pH 7.5, 300 mM NaCl, 1 mM EDTA, 0.5% Triton X-100, 0.1% sodium deoxycholate, 0.1% SDS, and protease inhibitors); twice with 50 mM Hepes-KOH pH 7.5, 250 mM NaCl, 1 mM EDTA, 0.25% Triton X-100, 0.1% sodium deoxycholate, 0.05% SDS, and protease inhibitors; twice with 10 mM Tris-HCl pH 8.0, 0.25 M LiCl, 0.5% NP40, 0.5% sodium deoxycholate, and 1 mM EDTA; twice with 10 mM Tris-HCl pH 8.0, 0.25 M LiCl, and 1 mM EDTA; and once with TE (10 mM Tris-HCl pH 8.0 and 1 mM EDTA pH 8.0) at room temperature. Beads were eluted by incubating with 100 μl of 50 mM Tris-HCl pH 8.0, 10 mM EDTA, and 1% SDS at 65°C for 15 min. Eluates were transferred to a fresh tube and pooled with a final bead wash of 150 μl TE with 0.67% SDS. For input DNA, 200 μl TE with 1% SDS was added to 50 μl cell lysate extract. To reverse the cross-links, all samples were incubated at 65°C overnight, followed by the addition of 250 μl TE, 5 μg glycogen, and 100 mg proteinase K, and incubation at 37°C for 2 h. After adding 55 μl of 4 M LiCl, the samples were extracted once with phenol/chloroform and once with chloroform. DNA was then precipitated by two volumes of ethanol, washed with 75% ethanol, air dried, and resuspended in 50 μl TE with RNase A (20 μg/ml for input DNA and 2 μg/ml for affinity-precipitated DNA) and incubated at 37°C for 1 h. Gel conditions, quantification of PCR amplified specific bands, and primer pairs—except for PCR1 of YBR079C: 5′TGAGCACGCTTCTGTCTTTC3′, 5′GAAGGCTGAATTGGAAGCTG3′ and PCR2 of YBR079C: 5′ACAGCGATTTTTCGATGTCC3′, 5′GGTTTTTGTTGCTGCCTCTC3′—were as previously described [20, 42].

Chromatin affinity-precipitation on chip (ChAP on chip)

The precipitated chromatin DNA fragments were obtained as described above. Then, following the NimblGen standard protocol instructions, samples were processed from the

steps of post IP, ligation-mediated PCR (LM-PCR), labelling with either cy5 or cy3, hybridization with *S. cerevisiae* whole genome tiling array chip (NimbleGen), to the step of scanning chip and analysis of data using the NimbleScan program and SignalMap software.

Results

Association of AAR with Sir2

Based on the ability of Sir2 to generate AAR, a Sir2-AAR interaction is postulated. However, intriguing as this proposed interaction is, a definitive proof is lacking. Therefore, we were interested to investigate the physical interaction between AAR and Sir2.

In order to obtain sufficient quantities of AAR, we optimized the condition of purification of AAR. We were able to produce AAR by enzymatic synthesis using either Sir2 or its homolog proteins, Hst2 and CobB (Fig. 1a). As shown in Fig. 1b, Sir2 was slightly more efficient in deacetylation of the substrate than Hst2 and CobB. Therefore, we chose Sir2 for the further large scale reactions. We also used thin layer chromatography (TLC) to monitor the results of the enzyme reaction over time. Under our conditions, after 2 and 12 h, around 54 and 85% of NAD was metabolized to AAR and NAM by Sir2, respectively. After 20 h reaction, there was still about 5% unconsumed NAD (Fig. 1c). As previously described [30], we purified the reaction products on a C18 HPLC column. Two peaks of interest, one containing AAR and the other containing AAR and NAD, were individually collected (Fig. 1d). The pure AAR peak collections were then combined, checked, and re-purified by HPLC again (Fig. 1e) and also confirmed by matrix assisted laser desorption/ionization-time of flight (MALDI-TOF) mass spectrometry (Fig. 1f).

We used a dot blotting assay to rapidly determine the physical binding of AAR to Sir2 that was immobilized on a PVDF membrane. We blotted increasing amounts of each protein (50–200 μmol) onto membranes, which were then incubated with ^{32}P-labeled AAR. As shown in Fig. 2a, consistent with the Hst2-AAR crystal structure [57], we detected binding of AAR to Hst2, even for the lowest Hst2 concentration (50 μmol) on the membrane. In the control, we observed no binding to BSA and C-terminal fragment of Sir3 at the same concentration range (data not shown). AAR also associated with Sir2 with an apparently higher efficiency than with Hst2 (Fig. 2a).

For studying the specificity of small molecule interaction with protein, we used an affinity pull-down approach. Several small molecules such as NAD, ADP-ribose (ADPR), nicotinamide (NAM), ATP, ADP, AMP, and AAR were immobilized on solid resins, which were then used to examine the specificity of affinity pull-down. Sir2 and Hst2 associated with AAR, as well as NAD, but bound little or no ATP, ADP, or AMP (Fig. 2b, c and data not shown). Furthermore, not only yeast Sir2 and Hst2 but human SirT1 were also able to undergo affinity pull-down by AAR but not by AMP from whole cell lysate extract (Fig. S1). Nevertheless, Sir2 associated with ADPR with a similar efficiency to that observed for AAR. Sir2 associated with NAM with lower efficiency. Both association of Hst2 with ADPR and with NAM showed a lower efficiency than Hst2-AAR association.

To measure the real time binding of small molecule interaction with Sir2, we performed BIAcore surface plasmon resonance (SPR) assays. Sir2 and control BSA were individually immobilized to a CM5 sensor chip, and small molecules were then used as the analyzers. Binding was observed between Sir2 and AAR but not between Sir2 and ADP or Sir2 and AMP (Fig. 2d and data not shown). The on and off rates for the association of AAR, ADPR, NAD, ADP, and AMP with Sir2 are summarized in Table 1. Affinity calculation yielded K_D values of ~300 nM for the Sir2-AAR interactions. The K_D value for the association of NAD

with Sir2 was ~580 nM. However, ADPR bound to Sir2 with lower affinity (K_D of ~3 μM) (Table 1).

Affinity precipitation of heterochromatin fragments by AAR

Chromatin immunoprecipitation (ChIP) (19) has allowed significant progress in the study of in vivo protein-DNA interactions. We modified the typical ChIP protocol to assess the ability of small molecules such as AAR, NAD, and ATP to associate with sheared chromatin fragments. Briefly, this method, referred to as chromatin affinity-precipitation (ChAP) involves the immobilization of small molecules to an Affigel resin via primary amine cross-linking. This resin is then used for affinity-precipitation and analysis of chromatin fragments as is the case with the standard ChIP assay.

Under our experimental conditions, as shown in Fig. 3a and b, using actin as a control, we observed enrichment signals of silent chromatin fragments, HMR-E, HML-E, HMR-a, HML-*a*, NTS1/5S, and NTS2/18S, using the AAR resins compared to resins that contained either ATP or other small molecules (about 1.5- to 2- vs. 1-fold enrichment over input). Interestingly, for NAD, the enrichment signals were detected on HMR-E, NTS1/5S, and NTS2/18S but not on HML-E, HMR-a, and HML-*a*. In contrast, for ADPR, the enrichment signals were detected on HMR-E, HML-E, HML-*a*, NTS1/5S, and NTS2/18S but not on HMR-a. AAR-dependent DNA precipitation required chromatin, as no enrichment was observed using naked DNA fragments (Fig. 3c). These results indicated that we were able to specifically precipitate silent heterochromatin fragments using the distinct immobilized small molecules such as AAR.

Previous studies have shown that deletion of any of the *sir* genes results in a disruption of heterochromatin [1, 18, 41]. To determine whether the association of AAR with chromatin required heterochromatin formation, we performed ChAP assays in wild type cells and cells that carried a deletion of the *sir2* gene. As our results suggest that Sir2 is an AAR binding partner, AAR should not be able to affinity-precipitate silent chromatin fragments in *sir2* deletion cells. As shown in Fig. 4, we observed an enrichment of four different silent chromatin fragments, the HMR-E and HML-E silencers, the HMR-a, and HML-*a* regions in ChAP from two different *sir2*$^+$ strains, but these enrichments were not detected in *sir2* deletion cells. No significant difference in the signal enrichment of the above fragments was observed between *sir2*$^+$ and *sir2* deletion cells in ChAP assays with AMP beads (Fig. 4). Although the enrichment of silent chromatin fragments in AAR pull-downs appeared to be weak (about 1.5-fold enrichment over input), the dependence on Sir2 suggested specificity in this assay. The association of AAR with silent chromatin fragments was consistent with our binding results presented in Fig. 2.

Genome-wide localization of AAR and Sir2

We next used the ChAP and ChIP assays in combination with whole genome tiling array chips to determine the genome-wide localization of AAR and Sir2. Genome-wide localization of Sir2 has been previously reported [28], but not using high resolution tiling arrays (“microarray of ~13 k unique spots at a resolution of 2 kb” vs. “tiling array of 385 kb probes with 50-mer probes at 32 bp median spacing”).

In general, AAR co-localized with Sir2 not only at all telomeric regions but also at almost all other chromosomal regions (Figs. 5 and S2). Interestingly, at several chromosome ends, including 1L, 1R, 2R, 3L, 3R, 4L, 6R, 9R, 10R, 11L, 11R, 13R, 14R, and 15L, both Sir2 and AAR display a narrower localization pattern (around only 1 kb from the terminus) compared to their distributions on other chromosomal ends (Fig. 5b). However, the localizations of Sir2 and AAR on each chromosome end ranged from ~1 to ~14 kb and, moreover, the

broader distribution regions displayed a closely connected bi- or tri-peak distribution pattern (Figs. 5a, b and S2).

We performed further data analysis by calculating and filtering out peaks with false discovery rate (FDR) by using NimbleScan software. Other than the known silent chromatin regions, this analysis identified 312 potential AAR association clusters that spanned 481 genes, about 6.7% of yeast genes, and 40 intergenic regions (Table S1). We also used the PCR method to confirm some of these newly identified AAR association gene regions (Fig. S1), and the results were consistent with our ChAP on chip results. However, these newly identified cluster regions were mostly co-associated with Sir2 (Figs. 5 and S2). Interestingly, at some regions, we observed AAR association in the apparent absence of Sir2, particularly near the end parts of cluster distribution (e.g., Chromosome 2, ~397 k, Fig. 5c), suggesting that the association may be mediated by other AAR receptor proteins in these regions. This feature was consistent with the PCR results shown in Fig. 5d. We also confirmed this co-association feature by using *sir2* deletion cells and almost all enrichment signals of AAR and Sir2 disappeared, except a few weak enrichment signals on some regions, such as YIR019C (Figs. S2 and S3). However, compared to the telomeric DNA regions, in which the highest enrichment was over 30-fold in Sir2 immunoprecipitations, these newly identified regions were usually enriched less than 8-fold (the cut-off of enrichment fold was artificially set at $2^{1.5}$ for the threshold value of AAR affinity-precipitation) (Figs. 5 and S2). As shown in supplemental Table S2, these AAR-associated regions were diverse and contained genes involved in many biological functions such as transferase activity, transcription regulation, protein binding, DNA binding, and signal transduction. At the same time, other ontological analyses of, for example, biological processes and cellular components also showed a similar diversity. However, it remains to be determined whether the Sir2 protein and AAR play any role in the regulation of these loci.

Our results showed that all chromosome ends were associated with Sir2 (Figs. 5a and S2), whereas previously little or no Sir2 enrichment was observed for telomeric regions of chromosomes 3R, 4L, 9R, and 16R [28]. However, most of the previously identified nonheterochromatic targets of Sir2 [28] were also enriched in our tiling array experiments (Fig. 5, Table S2).

Discussion

Our results show that the ChAP method provided a general useful assay for studying the association of small molecules with chromosomal DNA fragments. Using ChAP assay, we have provided direct physical evidence for the interaction of a small metabolic molecule, AAR, with the Sir2.

Both AAR-Sir2 and AAR-Hst2 interactions are consistent with the known ability of these enzymes to use NAD as a cofactor during deacetylation and with the observation that NAM is an inhibitor of Sir2 [3]. Presumably, the binding of AAR to Sir2 and Hst2 reflects its affinity for the known NAD binding pocket in the active site of these enzymes [2, 56, 57]. However, our results do not rule out the possibility that AAR association with chromatin fragments involves a Sir2-mediated heterochromatin formation.

Although AAR is produced by Sir2-like proteins from bacteria, yeast, and humans, its biological target(s) are not fully known. One of the nuclear sirtuins, Hst2, a Sir2 homolog in yeast, has been shown to co-crystallize with both AAR and a histone peptide [57]. A histone variant macroH2A1.1, mH2A1, has been identified as a target of ADP-ribose and/or AAR binding [24].

The phylogenetic conservation of Sir2-like enzymes and their reaction mechanism suggests that AAR may play similar regulatory roles in other systems. Sir2-like proteins have been implicated in several different regulatory pathways, and in mammalian systems, the SirT1 protein deacetylates p53, tubulin, and PCAF [4, 7, 10, 11]. AAR had been reported to directly bind to the cytoplasmic domain of TRPM2 and to activate the TRPM2 channel [15]. Furthermore, a recent report showed that AAR binds to three glycolytic enzymes, GAPDH, PGK, and ADH, suggesting that AAR may be involved in the cytosolic regulation of glycolysis [51]. AAR, whose production is coupled to deacetylation of these and as yet to be identified substrates, may act as a signaling or second messenger molecule to regulate downstream events. In this regard, AAR may be similar to cyclic ADP-ribose (cADPR), which is a second messenger that regulates calcium signaling in mammalian cells [17].

On the whole genome tiling array chip, at several chromosome ends, such as 4L, 9R, and 11R (Fig. 5b), an absence of Sir2 and AAR broader spreading along the chromosomal end was shown. This might imply that Sir2 was just involved in a short distance (~1 kb) of spreading but not further longer spreading at these telomeres. Under our experimental conditions, although Sir2 and AAR displayed similar genomic distribution patterns, some regions only associated with either Sir2 or AAR (Figs. 5c and S1), suggesting that AAR might not associate with all Sir2 interaction regions. Perhaps, other chromosome-bound Sir2-like proteins, such as Hst1, mediate the association of AAR with these chromosome regions.

It has been reported that the requirement for Sir2 and AAR in silencing can be bypassed when Sir3 is fused with Hos3 as a chimera protein [9] or when Sir3 is overexpressed in cells containing histone H4 lysine to arginine mutations that mimic deacetylated H4 [54]. Our studies provide a starting point for further dissection of the AAR binding site, which is required in order to assess the importance of AAR-Sir binding in silent chromatin assembly in vivo. Nevertheless, in addition to AAR interaction with Sir2, we have also found that AAR binds to Sir3 (unpublished data), suggesting that multiple interaction sites of the SIR complex may contribute to AAR binding.

The genome-wide ChAP approach described here is useful not only for identification of chromosome-associated AAR targets but also for the identification of non-chromosomal targets of AAR. In the nucleus, the results of genome-wide screening show that AAR primarily co-precipitates with genomic fragments that are associated with Sir2 (Figs. 5 and S2). However, some AAR-associated regions did not contain Sir2 (Fig. 5c) and may be bound by other AAR target protein(s), such as other Sir2-like proteins or Sir3. To fully investigate the possible biological function(s) of AAR, the identification of its other targets, including both nuclear and cytoplasmic targets, is required. Affinity precipitation using a small molecule coupled to a solid resin was used successfully to identify the first histone deacetylase [50]. AAR coupled to a solid resin, combined with mass spectrometry identification of the bound proteins, should be useful in identification of additional AAR targets.

Supplementary Material

Refer to Web version on PubMed Central for supplementary material.

Acknowledgments

We thank Drs. Yun-Shien Lee and Tina Fu for helpful discussion of chip analysis and lab members of G.-G.L. and of D.M. for discussion and technical help on this work. We also thank Yu-Hsin Kao of the Microarray Core Facility and Hsilin Cheng of the Mass Spectrometry Facility at the Institute of Molecular Biology, Academia Sinica for

technical assistance. This work was supported by grant number NSC-97-2311-B-400-001-MY3 to G.-G.L. and by a grant from the NIH to D.M. (GM61641). D.M. and T.W. are HHMI investigators.

References

1. Aparicio OM, Billington BL, Gottschling DE. Modifiers of position effect are shared between telomeric and silent mating-type loci in *S. cerevisiae*. Cell. 1991; 66:1279–1287. [PubMed: 1913809]
2. Avalos JL, Boeke JD, Wolberger C. Structural basis for the mechanism and regulation of Sir2 enzymes. Mol Cell. 2004; 13:639–648. [PubMed: 15023335]
3. Bitterman KJ, Anderson RM, Cohen HY, Latorre-Esteves M, Sinclair DA. Inhibition of silencing and accelerated aging by nicotinamide, a putative negative regulator of yeast Sir2 and human SIRT1. J Biol Chem. 2002; 277:45099–45107. [PubMed: 12297502]
4. Blander G, Guarente L. The Sir2 family of protein deacetylases. Annu Rev Biochem. 2004; 73:417–435. [PubMed: 15189148]
5. Borra MT, O'Neill FJ, Jackson MD, Marshall B, Verdin E, Foltz KR, Denu JM. Conserved enzymatic production and biological effect of *O*-acetyl-ADP-ribose by silent information regulator 2-like NAD^+-dependent deacetylases. J Biol Chem. 2002; 277:12632–12641. [PubMed: 11812793]
6. Bryk M, Banerjee M, Murphy M, Knudsen KE, Garfinkel DJ, Curcio MJ. Transcriptional silencing of Ty1 elements in the RDN1 locus of yeast. Genes Dev. 1997; 11:255–269. [PubMed: 9009207]
7. Carmen AA, Milne L, Grunstein M. Acetylation of the yeast histone H4 N-terminus regulates its binding to hetero-chromatin protein SIR3. J Biol Chem. 2002; 277:4778–4781. [PubMed: 11714726]
8. Cheung P, Allis CD, Sassone-Corsi P. Signaling to chromatin through histone modifications. Cell. 2000; 103:263–271. [PubMed: 11057899]
9. Chou C–C, Li Y-C, Gartenberg MR. Bypassing Sir2 and *O*-acetyl-ADP-ribose in transcriptional silencing. Mol Cell. 2008; 31:650–659. [PubMed: 18775325]
10. Denu JM. Linking chromatin function with metabolic networks: Sir2 family of NAD+-dependent deacetylases. Trends Biochem Sci. 2003; 28:41–48. [PubMed: 12517451]
11. Denu JM. The Sir2 family of protein deacetylases. Curr Opin Chem Biol. 2005; 9:431–440. [PubMed: 16122969]
12. Gaba A, Jacobson A, Schs MS. Ribosome occupancy of the yeast CPA1 upstream open reading frame termination codon modulates nonsense-mediated mRNA decay. Mol Cell. 2005; 20:449–460. [PubMed: 16285926]
13. Gasser SM, Cockell MM. The molecular biology of the SIR proteins. Gene. 2001; 279:1–16. [PubMed: 11722841]
14. Gottschling DE, Aparicio OM, Billington BL, Zakian VA. Position effect at *S. cerevisiae* telomeres: reversible repression of pol II transcription. Cell. 1990; 63:751–762. [PubMed: 2225075]
15. Grubisha O, Rafty LA, Takanishi CL, Xu X, Tong L, Perraud A-L, Scharengerg AM, Denu JM. Metabolite of Sir2 reaction modulates TRPM2 ion channel. J Biol Chem. 2006; 281:14057–14065. [PubMed: 16565078]
16. Grundy FJ, Henkin TM. The T box and S box transcription termination control system. Fornt Biosci. 2003; 8:d20–d31.
17. Guse AH. Second messenger function and the structure-activity relationship of cyclic adenosine diphosphoribose (cADPR). FEBS J. 2005; 272:4590–4597. [PubMed: 16156781]
18. Hecht A, Strahl-Bolsinger S, Grunstein M. Spreading of transcriptional represser SIR3 from telomeric heterochromatin. Nature. 1996; 383:92–96. [PubMed: 8779721]
19. Hecht A, Strahl-Bolsinger S, Grunstein M. Mapping DNA interaction sites of chromosomal proteins crosslinking studies in yeast. Methods Mol Biol. 1999; 119:469–479. [PubMed: 10804533]
20. Huang J, Moazed D. Association of the RENT complex with nontranscribed and coding regions of rDNA and a regional requirement for the replication fork block protein Fob1 in rDNA silencing. Genes Dev. 2003; 17:2162–2176. [PubMed: 12923057]

21. Imai S, Armstrong CM, Kaeberlein M, Guarente L. Transcriptional silencing and longevity protein Sir2 is an NAD-dependent histone deacetylase. Nature. 2000; 403:795–800. [PubMed: 10693811]
22. Jenuwein T, Allis CD. Translating the histone code. Science. 2001; 293:1074–1080. [PubMed: 11498575]
23. Klar AJS, Fogel S, MacLeod K. *MAR1*—a regulator of the *HMa* and *HMα* loci in *Saccharomyces cerevisiae*. Genetics. 1979; 93:37–50. [PubMed: 17248968]
24. Kustatscher G, Hothorn M, Pugieux C, Scheffzek K, Ladurner AG. Splicing regulates NAD metabolite binding to histone macroH2A. Nat Struct Mol Biol. 2005; 12:624–625. [PubMed: 15965484]
25. Ladurner AG. Rheostate control of gene expression by metabolites. Mol Cell. 2006; 24:1–11. [PubMed: 17018288]
26. Landry J, Sutton A, Tafrov ST, Heller RC, Stebbins J, Pillus L, Sternglanz R. The silencing protein SIR2 and its homologs are NAD-dependent protein deacetylases. Proc Natl Acad Sci USA. 2000; 97:5807–5811. [PubMed: 10811920]
27. Lee S, Tong L, Denu JM. Quantification of endogenous sirtuin metabolite *O*-acetyl-ADP-ribose. Anal Biochem. 2008; 15:174–179. [PubMed: 18812159]
28. Lieb JD, Liu X, Botstein D, Brown PO. Promoter-specific binding of Rap1 revealed by genome-wide maps of protein-DNA association. Nat Genet. 2001; 28:327–334. [PubMed: 11455386]
29. Liou G-G, Chang HY, Lin CS, Lin-Chao S. DEAD box RhlB RNA helicase physically associates with exoribonuclease PNPase to degrade double-stranded RNA independent of the degradosome-assembling region of RNase E. J Biol Chem. 2002; 277:41157–41162. [PubMed: 12181321]
30. Liou G-G, Tanny JC, Kruger RG, Walz T, Moazed D. Assembly of the SIR complex and its regulation by *O*-acetyl-ADP-ribose, a product of NAD-dependent histone deacetylation. Cell. 2005; 121:515–527. [PubMed: 15907466]
31. Martino F, Kueng S, Robinson P, Tsai-Pflugfelder M, van Leeuwen F, Ziegler M, Cubizolles F, Cockell MM, Rhodes D, Gasser SM. Reconstitution of yeast silent chromatin: multiple contact sites and O-AADPR binding load SIR complexes onto nucleosomes in vitro. Mol Cell. 2009; 33:323–334. [PubMed: 19217406]
32. Matthews KS, Nichols JC. Lactose repressor protein: functional properties and struccture. Prog Nucleic Acid Res Mol Biol. 1998; 58:127–164. [PubMed: 9308365]
33. Moazed D. Common themes in mechanisms of gene silencing. Mol Cell. 2001; 8:489–498. [PubMed: 11583612]
34. Moazed D, Johnson D. A deubiquitinating enzyme interacts with SIR4 and regulates silencing in *S. cerevisiae*. Cell. 1996; 86:667–677. [PubMed: 8752220]
35. Moazed D, Kistler A, Axelrod A, Rine J, Johnson AD. Silent information regulator protein complexes in *Saccharomyces cerevisiae*: a SIR2/SIR4 complex and evidence for a regulatory domain in SIR4 that inhibits its interaction with SIR3. Proc Natl Acad Sci. 1997; 94:2186–2191. [PubMed: 9122169]
36. Moretti P, Freeman K, Coodly L, Shore D. Evidence that a complex of SIR proteins interacts with the silencer and telomere-binding protein RAP1. Genes Dev. 1994; 8:2257–2269. [PubMed: 7958893]
37. Motta MC, Divecha N, Lemieux M, Kamel C, Chen D, Gu W, Bultsma Y, McBurney M, Guarente L. Mammalian SIRT1 represses forkhead transcription factors. Cell. 2004; 116:551–563. [PubMed: 14980222]
38. North BJ, Marshall BL, Borra MT, Denu JM, Verdin E. The human Sir2 ortholog, SIRT2, is an NAD +-dependent tubulin deacetylase. Mol Cell. 2003; 11:437–444. [PubMed: 12620231]
39. Onishi M, Liou G-G, Buchberger JR, Walz T, Moazed D. Role of the conserved Sir3-BAH domain in nucleosome binding and silent chromatin assembly. Mol Cell. 2007; 28:1015–1028. [PubMed: 18158899]
40. Richards EJ, Elgin SC. Epigenetic codes for heterochromatin formation and silencing rounding up the usual suspects. Cell. 2002; 108:489–500. [PubMed: 11909520]
41. Rine J, Herskowitz I. Four genes responsible for a position effect on expression from HML and HMR in *Saccharomyces cerevisiae*. Genetics. 1987; 116:9–22. [PubMed: 3297920]

42. Rudner AD, Hall BE, Ellenberger T, Moazed D. A non-histone protein-protein interaction required for assembly of the SIR complex and silent chromatin. Mol Cell Biol. 2005; 25:4514–4528. [PubMed: 15899856]
43. Rusche LN, Kirchmaier AL, Rine J. The establishment, inheritance, and function of silenced chromatin in *Saccharomyces cerevisiae*. Annu Rev Biochem. 2003; 72:481–516. [PubMed: 12676793]
44. Shore D. The Sir2 protein family: a novel deacetylase for gene silencing and more. Proc Natl Acad Sci USA. 2000; 97:14030–14032. [PubMed: 11114164]
45. Smith JS, Boeke JD. An unusual form of transcriptional silencing in yeast ribosomal DNA. Genes Dev. 1997; 11:241–254. [PubMed: 9009206]
46. Smith JS, Brachmann BC, Celic I, Kenna MA, Muhammad KS, Starai VJ, Avalos JL, Escalante-Semerena JC, Grubmeyer C, Wolberger C, Boeke JD. A phylogenetically conserved NAD+-dependent protein deacetylase activity in the Sir2 protein family. Proc Natl Acad Sci USA. 2000; 97:6658–6663. [PubMed: 10841563]
47. Strahl-Bolsinger S, Hecht A, Luo K, Grunstein M. SIR2 and SIR4 interactions differ in core and extended telomeric heterochromatin in yeast. Genes Dev. 1997; 11:83–93. [PubMed: 9000052]
48. Tanny JC, Moazed D. Coupling of histone deacetylation to NAD breakdown by the yeast silencing protein Sir2: evidence for acetyl transfer from substrate to an NAD breakdown product. Proc Natl Acad Sci. 2001; 98:415–420. [PubMed: 11134535]
49. Tanny JC, Kirkpatrick DS, Gerber SA, Gygi SP, Moazed D. Budding yeast silencing complexes and regulation of Sir2 activity by protein-protein interactions. Mol Cell Biol. 2004; 24:6931–6946. [PubMed: 15282295]
50. Taunton J, Hassig CA, Schreiber ST. A mammalian histone deacetylase related to the yeast transcriptional regulator Rpd3p. Science. 1996; 272:408–411. [PubMed: 8602529]
51. Tong L, Lee S, Denu JM. Hydrolase regulates NAD^+ metabolites and modulates cellular REDOX. J Biol Chem. 2009; 284:11256–11266. [PubMed: 19251690]
52. Turner BM. Histone acetylation and an epigenetic code. BioEssays. 2000; 22:836–845. [PubMed: 10944586]
53. Winkler WC, Breaker RR. Regulation of bacterial gene expression by riboswitches. Annu Rev Microbiol. 2005; 59:487–517. [PubMed: 16153177]
54. Yang B, Kirchmaier L. Bypassing the catalytic activity of SIR2 for SIR protein spreading in *Saccharomyces cerevisiae*. Mol Biol Cell. 2006; 17:5287–5297. [PubMed: 17035629]
55. Zhang J, Kaasik K, Blackburn MR, Lee CC. Constant darkness is a circadian metabolic signal in mammals. Nature. 2006; 439:340–343. [PubMed: 16421573]
56. Zhao K, Chai X, Clements A, Marmorstein R. Structure and autoregulation of the yeast Hst2 homolog of Sir2. Nat Struct Biol. 2003; 10:864–871. [PubMed: 14502267]
57. Zhao K, Chai X, Marmorstein R. Structure of the yeast Hst2 protein deacetylase in ternary complex with 2′-*O*-acetyl ADP ribose and histone peptide. Structure. 2003; 11:1403–1411. [PubMed: 14604530]

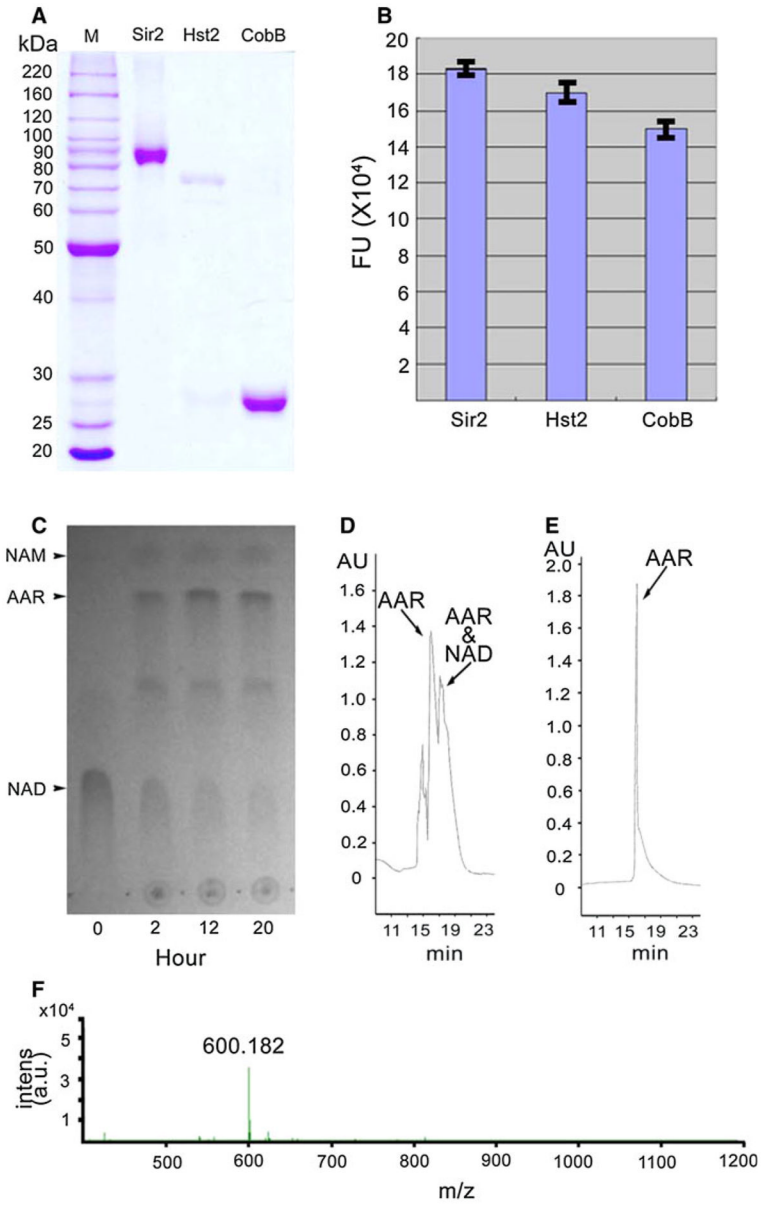

Fig. 1.

Purification of ARR. **a** Coomassie-stained SDS polyacrylamide gel showing purified Sir2, Hst2, and CobB. **b** HDAC fluorescent activity assays showing the deacetylation activities of Sir2, Hst2, and CobB, respectively. **c** TLC separation of NAD-dependent deacetylation reaction products. The reaction times, reactant (NAD), and products (AAR and NAM) are indicated on the *bottom* and *left*, respectively. **d** Purification of NAD-dependent deacetylation reaction products on a C18 HPLC column. The peaks were collected and the positions of AAR and NAD as determined by MALDI-TOF mass spectrometry are indicated. **e** Several collected AAR peaks shown in **d** were combined to be re-purified by HPLC. **f** Mass spectrum showing the molecular mass of AAR from the peak shown in **e**

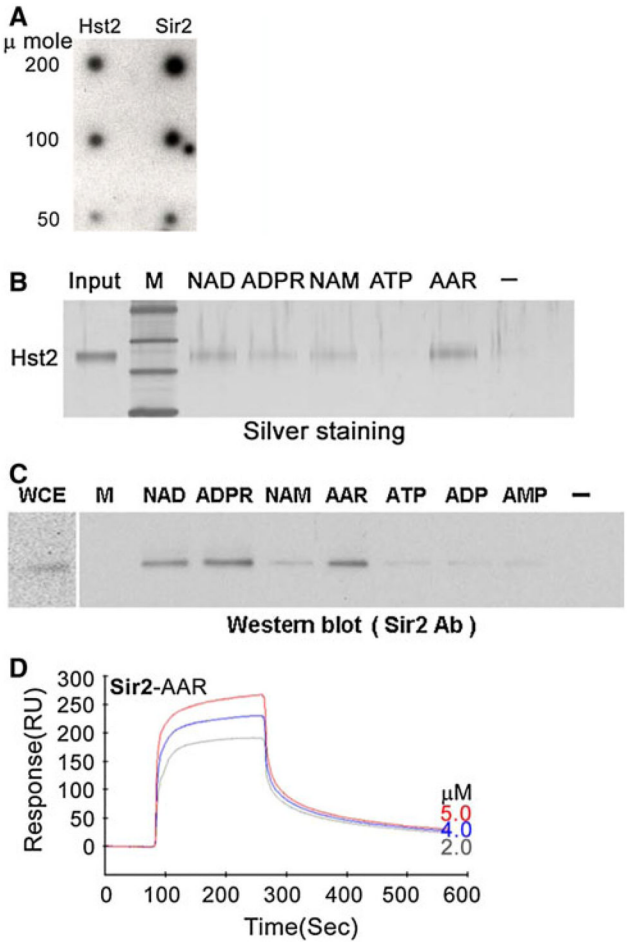

Fig. 2.

Association of small molecules with Hst2 and Sir2. **a** Dot blotting assays showing the binding of ^{32}P-AAR to the indicated amounts of Hst2 and Sir2 immobilized on a PVDF membrane. **b** and **c** Affinity pull-down assays showing the binding of Hst2 and Sir2 to the indicated small molecules, which were immobilized on beads. **d** BIAcore surface plasmon resonance (SPR) experiments showing the association of AAR with immobilized Sir2. The concentrations of AAR are indicated on the sensorgram (*right*). *M* Protein standard marker, *WCE* whole cell extract, – bead only control

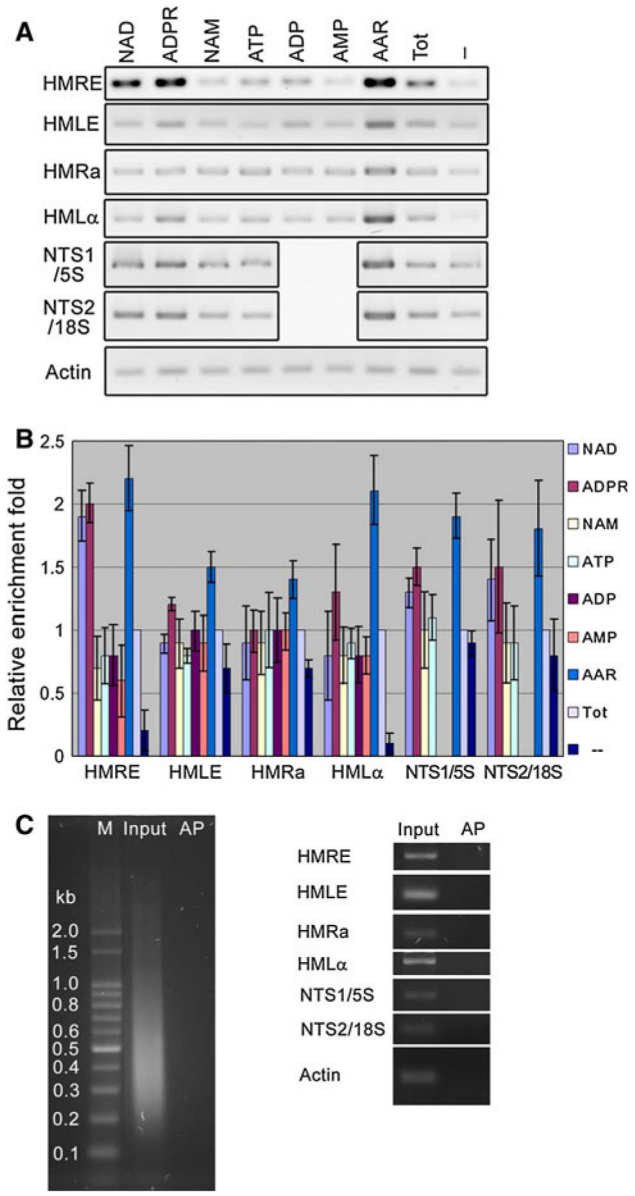

Fig. 3.

Chromatin affinity-precipitation (ChAP) assays. **a** Examples of the ChAP data used to determine the association of small molecules with silent heterochromatin fragments. Actin primer was used as internal control and for normalization of signal. **b** Quantifi-cation of ChAP experiments showing the relative fold enrichments of small molecules at each silent chromatin fragment. Averages and standard errors are shown for the results of three to five experiments. **c** Control experiment showing that AAR was unable to directly interact with naked DNA fragments. The total purified naked chromatin DNA fragments of input and the pull-down of AAR were separated on an agarose gel (*left panel*). The detected signals of input and pull-down of AAR at silent chromatin fragments and actin control are shown (*right panel*). The small molecules and silent chromatin fragments are indicated. *M* and *AP* represent the protein standard marker and affinity pull-down, respectively

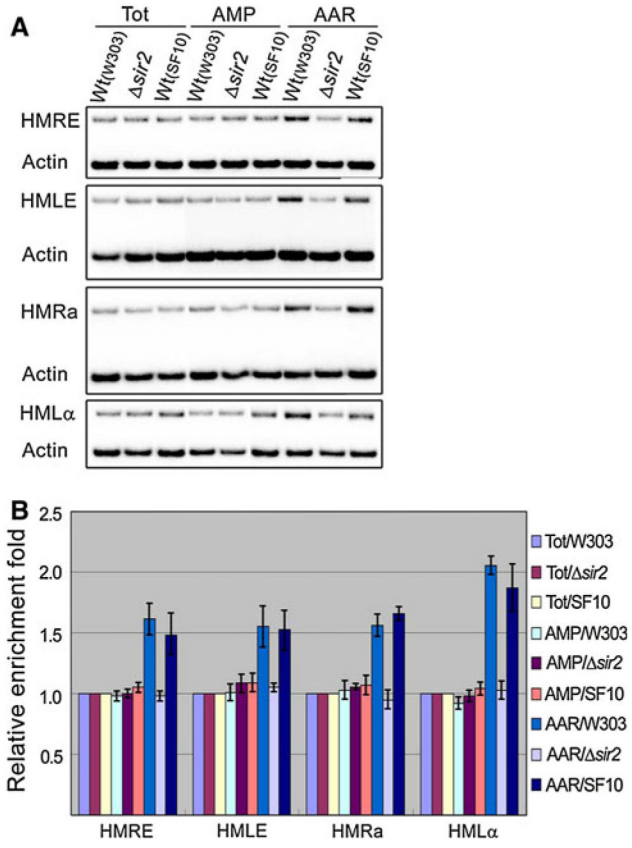

Fig. 4.

Sir2-dependent AAR association with silent chromatin. **a** ChAP assays showing the association of AAR with silent chromatin fragments in *sir2* deleted cells as compared with *sir2*$^{+}$ wild type cells. AMP was used as small molecule control, and actin primer was used as internal control and for normalization of signal. **b** Quantification of ChAP experiments showing the relative fold enrichments of AAR at silent chromatin fragments in *sir2*$^{+}$ and *sir2* deleted cells. Averages and standard errors are shown for the results of three to four experiments. *Tot*, *Wt(W303)*, *Wt(SF10)*, and *Δsir2* represent total cell lysate, two *sir2*$^{+}$ (wild type), and sir2 deleted strains, respectively

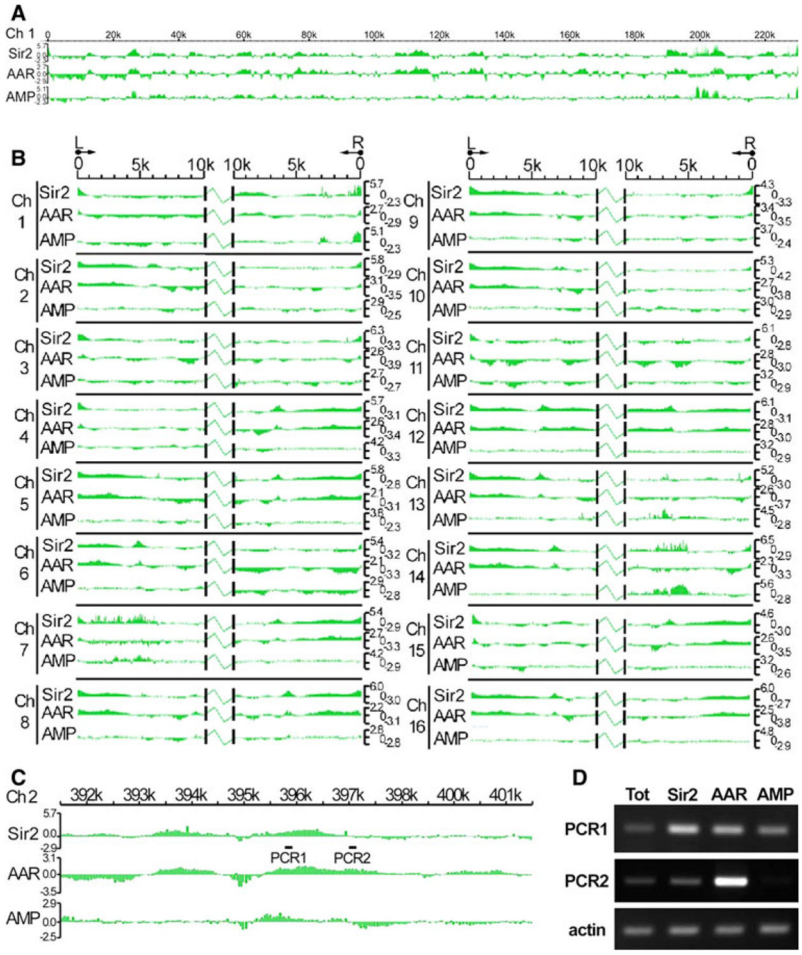

Fig. 5.

Genome-wide distribution of Sir2 and AAR. **a** Chromosomal display of association patterns of Sir2 and AAR on the whole chromosome 1. **b** Chromosomal display of association patterns on the telomere regions. For each chromosome, Sir2, AAR, and AMP data, respectively, are presented for the 10 kb region from the left (*L*) and right (*R*) chromosome end. **c** The different distributions of enrichment signals of Sir2 and AAR around position 397 k of chromosome 2. Chromosome number and the relative ratio of enrichment signal (log2) are indicated. **d** The different enrichment signals of Sir2 and AAR on the same region shown in **c**. The detected positions of PCR1 and PCR2 are also indicated in **c**. Actin primer was used as internal control and for normalization of signal. *Tot* represents total cell lysate

Table 1

Association of AAR, ADPR, NAD, ADP, and AMP with immobilized Sir2

Interaction	ka (1/Ms)	kd (1/s)	KD (M)
Sir2-AAR	$(1.23 \pm 0.02) \times 10^{3}$	$(3.74 \pm 0.35) \times 10^{-4}$	$(3.04 \pm 0.26) \times 10^{-7}$
Sir2-ADPR	$(8.17 \pm 0.06) \times 10^{2}$	$(2.41 \pm 0.12) \times 10^{-3}$	$(2.95 \pm 0.16) \times 10^{-6}$
Sir2-NAD	$(1.70 \pm 0.45) \times 10^{4}$	$(9.18 \pm 0.91) \times 10^{-3}$	$(5.75 \pm 1.33) \times 10^{-7}$
Sir2-ADP	NM	NM	NM
Sir2-AMP	NM	NM	NM

NM Not measurable